

# Island growth in submonolayer deposition with aggregation and fragmentation

M. Rusanen<sup>1,2,a</sup>, I.T. Koponen<sup>2</sup>, and J. Asikainen<sup>1,b</sup>

<sup>1</sup> Laboratory of Physics, PO Box 1100, 02015 HUT, Espoo, Finland

<sup>2</sup> Department of Physical Sciences, University of Helsinki, PO Box 64, 00014 University of Helsinki, Finland

Received 28 May 2003 / Received in final form 4 September 2003

Published online 30 January 2004 – © EDP Sciences, Società Italiana di Fisica, Springer-Verlag 2004

**Abstract.** Island growth is studied in the case of island aggregation and break-up during submonolayer deposition. It is demonstrated that the island size distributions are of the scaling form and the mean island size has a power-law behaviour corresponding to hyperthermal deposition conditions. The corresponding scaling exponents are analytically derived and compared with the simulations by the revised particle coalescence method developed here. The scaling exponents are found to depend only on the homogeneity exponents of aggregation and fragmentation kernels.

**PACS.** 68.55.-a Thin film structure and morphology – 68.35.Fx Diffusion; interface formation – 36.40.Sx Diffusion and dynamics of clusters

## 1 Introduction

Surface growth in the submonolayer regime proceeds via adatom deposition onto a surface, nucleation of adatom islands, and gradual growth of these islands at low coverages. In this growth regime a wealth of information about the effects of various microscopic processes can be obtained from the distribution of island sizes, the average island size, and the average areal density of islands. In most studies the focus has been on adatom diffusion [1–3], island mobility [4–6], and reversible aggregation through adatom detachment from islands [7–9]. The effect of island fragmentation or breakup on growth has been described as well [10]. It has been suggested that each of the above mentioned processes can have effects in practical deposition conditions, such as ion beam assisted deposition (IBAD) [11] and low energy ion deposition (LEID) [8,9,12]. Using standard Molecular Beam Epitaxy descriptions in the hyperthermal deposition leads to severely restricted predictions already on a qualitative level. For example, the size distributions are broader and the scaling exponents for the mean island size are different in hyperthermal case as compared with thermal deposition [8,12]. During hyperthermal deposition island breakup or fragmentation may be one of the processes affecting growth, e.g. by increasing the density of small is-

lands. On the other hand, creation of additional nucleation sites [11] and enhanced adatom detachment from islands may have similar consequences on growth [12]. The effects of microscopic processes on observable features of growth are, however, not yet fully understood in the case of island aggregation and fragmentation. The importance of these processes can be examined by using the reaction-rate description and rate-equations, which have turned out to be a powerful approach in surface growth problems [1–3].

In order to clarify the role of island breakup and diffusion on growth we concentrate here on a model system where other processes are omitted. In that, rate equation approach is used. Although the model including only aggregation through island diffusion, island fragmentation, and adatom deposition is not itself directly applicable to a real deposition system, it enables us to study the scaling relations of the mean island size and the size distributions. Detailed information about the scaling properties is, however, needed in order to differentiate the effects of island diffusion and fragmentation from other processes of interest in real experimental situations. Some of the features of growth specific to island diffusion and fragmentation may thus become accessible to experimental verification through these scaling properties, once the generic behaviour of all microscopic processes are known.

We have previously studied the problem of island growth where island aggregation and fragmentation have been taken into account [10], but several open questions remained. The present paper augments and completes the previous study by giving analytical estimates for the scaling exponents for the mean island size and the scaling

---

<sup>a</sup> *Present address:* Institut Français du Pétrole, Groupe de Modélisation Moléculaire, BP 311, 92852 Rueil-Malmaison, France; e-mail: Marko.Rusanen@ifp.fr

<sup>b</sup> *Present address:* HRS F27, ETH Zentrum, 8092 Zürich, Switzerland

function of the size distributions. Moreover, we describe a revised simulation method to numerically solve rate equations. The revised method facilitates to span a large range in the parameter space needed for the accurate estimates of the scaling exponents. We compare the analytical predictions both with the simulations using the revised method and numerical integration of the equation for the mean size. In both cases we find a good agreement.

## 2 Model system, rate equations, and scaling

The model system studied is reversible island growth, where islands are allowed to diffuse and break-up during growth. The purpose of the model is not to accurately describe a real deposition process but instead to clarify the generic features of growth in the presence of island diffusion and break-up. When scaling properties of such a model are known, it becomes possible to judge, whether real systems exhibit similar characteristic features.

The island diffusion model employed is island size dependent, following a simple power-law. This kind of island diffusion is observed in metallic systems [13,14]. Although the timescale for substantial movement of islands appears to be much larger than the timescale of deposition, it still can be expected to affect growth because even moderate movement may lead to enhanced coalescence of islands (for estimates of timescales see e.g. Ref. [6]). Also in kinetic Monte Carlo simulations mobilities of large islands are seen to affect growth [5], an observation now established by more idealized but yet phenomenologically relevant simulations [4,6].

The fragmentation model introduced here, however, may be of relevance in high enough deposition energies in LEID exceeding 30–50 eV or in IBAD with energies up to 100 eV. There is, however, no direct evidence of supported cluster fragmentation, because it is not easily available by experimental probes. Observations on related phenomena of fragmentation of sputtered clusters [15,16] suggest, that also clusters on surfaces break-up under energetic ion bombardment. It is also known that large island boundary fluctuations – certainly promoted by ion bombardment – lead to fragmentation of islands. In this case, the distribution of fragments is a slowly decreasing function of island size [16].

Although the models of fragmentation and island diffusion are too idealized for detailed description of real deposition systems, they contain qualitatively relevant information for clarifying the generic properties of growth and resolving its scaling properties. In real deposition systems, moreover, many other processes may appear to be more relevant. Detachment of single atoms from islands may be more important than fragmentation, detachment may mask the effects of diffusion of small islands [17], oscillations in diffusivity of small islands may be more significant, and in practice only dimers and trimers could be mobile enough to substantially affect growth [18]. All these details are omitted from the present model, because their inclusion would hinder the quantification and the classification of the effects of island fragmentation and mobility.

Reversible island growth, with diffusion and fragmentation as outlined above, can be described rather accurately neglecting the spatial correlations between growing islands [4,19,20] (for estimates of time scales, see Ref. [21]). The possibility to neglect the spatial correlations means that island growth with mobile islands and breakup can be modelled by using rate equations as a reversible aggregation-breakup process  $A_i + A_j \rightleftharpoons A_{i+j}$  of clusters of size  $i$  and  $j$  with the rates of aggregation and breakup specified by the reaction kernels  $K(i, j)$  and  $F(i, j)$ , respectively. The rate equations for the areal density  $n_s$  of islands of size  $s \geq 1$  in the system with incoming particle flux  $\Phi$  are given by [10]

$$\frac{dn_s}{dt} = \Phi \delta_{1,s} + \frac{1}{2} \sum_{i+j=s} [K(i, j)n_i n_j - F(i, j)n_s] - \sum_{j=1}^{\infty} [K(s, j)n_s n_j - F(s, j)n_{s+j}]. \quad (1)$$

The aggregation kernel for mobile islands with the diffusion coefficient  $D_i$  is given by  $K(i, j) = K_0(D_i + D_j)$  for an island of size  $i$ , where the logarithmic size corrections [4] are ignored, consistently with the point island approximation used here. In many experimental realizations the diffusion coefficient follows a power law  $D_i \sim i^{-\mu}$ , which leads to the homogeneous aggregation kernel  $K(i, j) = K_0(i^{-\mu} + j^{-\mu})$ , where  $1 \leq \mu \leq 2$  [14]. It must be noted that there is some evidence [22] that for small clusters the effective exponent  $2 < \mu < 3$ , but since these results are inconclusive, we restrict our study to the former case only. The fragmentation kernel  $F(i, j)$  of an island of size  $s = i + j$  is also taken to be of the homogeneous form  $F(i, j) = F_0(i + j)^\alpha$ . Only binary breakup is allowed, which with  $-1/2 \leq \alpha \leq 0$  is a reasonable choice for hyperthermal deposition [23]. It must be emphasized that the homogeneity exponents  $\mu$  and  $\alpha$  are the only input parameters in the model, in addition to the ratios  $\mathcal{R} = K_0/\Phi$  (diffusion/deposition) and  $\kappa = F_0/K_0$  (fragmentation/diffusion).

The complete analytical solution to the rate equations (1) is not possible, but valuable information and properties of the solutions can be obtained through the scaling arguments. In irreversible island growth it is well known that  $\bar{s} \sim \mathcal{R}^\gamma \theta^\beta$  with  $\gamma = 1/3$  and  $\beta = 2/3$  for point islands [2], where the mean island size is  $\bar{s} = \sum_{k \geq 2} k^2 n_k / \sum_{k \geq 2} k n_k$ , and  $\theta = \sum_k k n_k$  is the fractional coverage of islands. It should be noted that there are somewhat different conventions to define the mean island size [3,24]. These definitions, however, are essentially equivalent since they lead to the same scaling relations. Our choice is convenient for the scaling of the distribution  $p(x)$  defined below. In aggregation with fragmentation without deposition the mean size behaves differently from irreversible growth, and it is found that  $\bar{s} \sim \kappa^y$  with  $y = 1/(\mu + \alpha + 2)$  [25]. The two scaling forms of irreversible growth and aggregation with fragmentation can be combined into the single scaling form for the mean size [10]:

$$\bar{s} \sim \theta^y \Psi(\theta), \quad (2)$$

where  $\Theta = \theta/\theta_c$ ,  $\theta_c = \mathcal{R}^{-\gamma/(\beta-y)}\kappa^{-y/(\beta-y)}$ . The scaling function  $\Psi(\Theta)$  behaves as  $\Psi \sim \Theta^{\beta-y}$  for  $\Theta \ll 1$ , and  $\Psi \sim \text{const.}$  for  $\Theta \gg 1$ .

The size distributions are expected to scale in the quasi-stationary regime, where the only length scale is  $\bar{s}$ . We previously showed [10] that the scaling form similar to island growth holds [2,3,24]:

$$n_s(\theta) = \frac{\theta}{\bar{s}^2} f(s/\bar{s}), \quad (3)$$

where  $f(x)$  is a scaling function. It is convenient to introduce a function  $g(x) = xf(x)$  describing the scaling of the distribution  $p(s, \theta) = sn_s(\theta)/\theta$ . This distribution can be understood to be equal to the probability that a randomly chosen adatom is contained in an island of size  $s$  [3,25]. We suggested [10] that  $g(x)$  has the form  $g(x) \sim x^\delta \exp(-ax)$ , where  $a$  is constant and  $\delta$  is a scaling exponent, similar to aggregation with fragmentation [19]. After an initial transient stage the scaling function becomes independent of coverage and of the parameters  $\mathcal{R}$  and  $\kappa$ .

### 3 Revised particle coalescence method

The numerical solutions to the rate equations (1) can be obtained using the particle coalescence method (PCM) simulations [20]. In PCM islands are considered as point-like objects, which grow by aggregating other islands and adatoms with the probabilities specified by the aggregation kernel  $K(i, j)$  between islands of sizes  $i$  and  $j$ . The islands are located on a lattice which does not correspond to a physical lattice (so the symmetry is irrelevant), but only represents an island size distribution at the given coverage. This implies that the PCM approach simulates the growth problem at a mean-field level, where all correlations between islands are neglected. The point-island approximation holds at small coverages and allows one to define the reaction kernels in the rate equations exactly since the geometric effects arising from the complicated morphology of real islands are not taken into account.

Island growth with aggregation through island diffusion, island fragmentation, and adatom deposition can be simulated with PCM as follows. An island is randomly chosen and its break-up is tested with the probability given by the fragmentation kernel  $F(i, j)$ . If the fragmentation event fails, an attempt is made to move it into a random position on the lattice. If this site is empty, the island jumps with probability 1, otherwise an attempt for an aggregation event is made with the probability specified by the reaction kernel  $K(i, j)$ . An adatom is deposited onto a random site after every  $1/\Phi$  steps.

In PCM the spatial variations in the island density are neglected, which is implemented by allowing islands to jump into empty lattice sites. The drawback of this method is that most of the events during the simulation only mix the system, and only a small fraction of all events contribute to the evolution of the size distribution. This leads to long simulation times, e.g. when  $\mathcal{R}$  is increased. The efficiency of PCM simulations can be improved by

removing the unnecessary jumps into empty sites as described below.

In the traditional Metropolis Monte Carlo algorithm, one chooses a transition with the uniform probability  $1/N$ , where  $N$  is the number of possible transitions from the initial configuration. The transition is then accepted with the probability  $\nu_{i \rightarrow f}/\nu_{\max}$ , where  $\nu_{i \rightarrow f}$  is the transition probability from the initial state  $i$  to the final state  $f$ , and  $\nu_{\max}$  is the maximum of all transition rates. The time is then incremented by constant steps. It has been shown, however, that the time can be advanced stochastically also in Metropolis-type algorithms [26]. In this case the total transition rate is given by  $\Gamma_M = N\nu_{\max}$ , and the time step  $\Delta t$  is drawn from the distribution  $\Gamma_M \exp(-\Gamma_M \Delta t)$ , whether the attempt to change the configuration is successful or not [26]. The problem is to find  $\Gamma_M$  appropriate for the system.

The transition rate  $\Gamma_M$  in island growth with aggregation, fragmentation, and deposition can be found as follows. The total number of possible aggregation events is  $N_{\text{aggr}} = N_{\text{isl}}(N_{\text{isl}} - 1)$ , where  $N_{\text{isl}}$  is the total number of islands. Total number of possible fragmentation events is  $N_{\text{frag}} = N_{\text{isl}}$ , since all islands are allowed to break-up. Denoting the incoming monomer flux by  $\Phi$  in units of monolayers per second, the flux rate is given by  $L^2\Phi$  (corresponding a two-dimensional system), where  $L$  is the linear system size.

The crucial step is to remove the jumps into empty sites. This implies that the relative rate of the aggregation events is increased, which has to be balanced in the other rates. The correction term is given by the number of empty sites in the original lattice  $L^2 - N_{\text{isl}}$ , which is equal to the number of possible island jumps into a empty site in the old PCM. The correct fragmentation and deposition rates are then given by  $\Gamma_F = \nu_{\text{frag}}^{\max} N_{\text{isl}}(L^2 - N_{\text{isl}})$  and  $\Gamma_D = L^2\Phi(L^2 - N_{\text{isl}})$ , respectively, while the aggregation rate  $\Gamma_A = \nu_{\text{aggr}}^{\max} N_{\text{isl}}(N_{\text{isl}} - 1)$ .

Disregarding the jumps into empty sites, one needs only a list containing all islands and their sizes. If an aggregation event is chosen, one picks randomly two islands from the list and makes an attempt to aggregate them with the probability  $K(i, j)$ . If a fragmentation event is chosen, one island is randomly attempted to break-up with the probability  $F(i, j)$ . It should be kept in mind that the maximum rates can depend on the form of the reaction kernels. For example, for  $F(i, j) = F_0(i+j)^\eta$  where  $\eta > 0$ ,  $\nu_{\text{frag}}^{\max}$  depends on the largest island in the system.

### 4 Results

The scaling exponents can be obtained from the rate equation (1) together with the scaling ansatz for the size distributions. Equation (1) are multiplied by  $s^2$  and summed over  $s$ . In the asymptotic limit  $s, \bar{s} \rightarrow \infty$ ,  $x = s/\bar{s} = \text{const.}$ , one converts the sums into the corresponding integrals and assumes that all integrals converge. The resulting equations can be separated into time-dependent and  $x$ -dependent parts giving the scaling exponents in the initial and final stage of growth. These exponents, defined in

**Table 1.** Simulation results for the scaling exponents of the mean island size and the scaling function of the size distributions are shown. The values for the exponents are given by the analytical values from the rate equations (RE) and the simulations (PCM). Errors in measured values are 0.05 in  $\beta$ , 0.02 in  $\gamma$ , and 0.05 in  $\delta$ .

$(\mu, \alpha)$	$\beta$		$\gamma$		$\delta$	
	RE	PCM	RE	PCM	RE	PCM
$(2, 0)$	0.66	0.72	0.33	0.34	3.00	2.93
$(2, -\frac{1}{2})$	0.66	0.71	0.33	0.33	2.50	2.35
$(1, 0)$	1.00	1.02	0.50	0.51	2.00	2.00
$(1, -\frac{1}{2})$	1.00	1.03	0.50	0.50	1.50	1.49

Section 2, are given by

$$\begin{aligned}
 \beta &= 2/(\mu + 1), \\
 \gamma &= \beta/2, \\
 \delta &= \mu + \alpha + 1, \\
 y &= 1/(\mu + \alpha + 2).
 \end{aligned}
 \tag{4}$$

To our knowledge the results for  $\beta$  and  $\gamma$  are new, while the values of  $\delta$  and  $y$  are the same as in aggregation with fragmentation [19, 25]. The analytical values are compared with the simulation results in Table 1, showing a good agreement.

Similarly to the derivation of the scaling exponents, from equation (1) follows the equation for the mean island size:

$$\frac{d(\theta\bar{s})}{d\theta} = \mathcal{R} [c_1\theta^{2+\mu}(\theta\bar{s})^{-\mu} - c_2\kappa\theta^{-\alpha-1}(\theta\bar{s})^{\alpha+2}] + 1, \tag{5}$$

where  $c_1$  and  $c_2$  are constants depending on the form of the reaction kernels  $K(i, j)$  and  $F(i, j)$ , respectively. The numerical integration of equation (5) gives a further support for the analytical value of the dynamic exponent. Figure 1 shows the resulting behavior of the scaling function with the model  $(\mu, \alpha) = (2, 0)$ . The scaling function has a power-law behavior for  $\Theta \ll 1$ , and it approaches a constant value for  $\Theta \gg 1$ . The inset shows the behavior of the dynamic exponent as a function of coverage. It decreases from the initial value given by  $\beta = 2/(\mu + 1)$  until the quasi-stationary regime is reached, where  $\bar{s} \sim \theta^y$ .

The analytical estimates (4) for the scaling exponents were confirmed with the revised PCM simulations. Typically the parameters were in the ranges  $10^5 \leq \mathcal{R} \leq 10^8$  and  $10^{-6} \leq \kappa \leq 10^{-3}$ , using 5000 averages for small  $\kappa$ , and 2000 averages for the largest  $\kappa$ . For small  $\kappa$  one can do easily  $\mathcal{R} = 10^9$  within a reasonable computation time. The simulations show that  $\bar{s}$  has a power-law behavior with the dynamic scaling exponent  $\beta$  in the initial stage and the exponent  $y$  in the aggregation-fragmentation dominated regime. In the simulations it was found that  $\beta$  depends only on island mobility for  $0 \leq \mu < 2$  and large enough fragmentation rate. We also confirmed the validity of  $\beta = 2/(\mu + 1)$  by performing few simulations with  $\mu = 0$ ,  $\mu = 1/2$ , and  $\mu = 3/2$  for small  $\kappa$ . However, the prediction for the dynamic exponent  $\beta$  applies only to mobile islands. The value  $\beta = 2/(\mu + 1)$  holds until  $\mu \approx 2$ ,

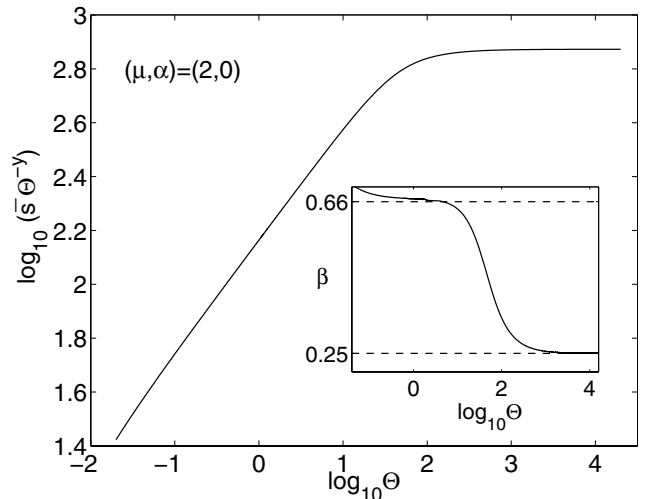


**Fig. 1.** The scaling function  $\Psi$  obtained from integration of the dynamic equation for the mean island size (Eq. (5)) is shown here in the case  $(\mu, \alpha) = (2, 0)$  (arbitrary units). The inset shows the behavior of the scaling exponent starting from the value  $\beta = 2/(\mu + 1) = 2/3$  and reaching the saturation value  $y = 1/(\mu + \alpha + 2) = 1/4$ . The dashed lines indicate the analytical values.

after which  $\beta = 2/3$  as predicted for immobile islands [2], consistent with the rate equations (1). The exponent  $\gamma$  is also found in simulations to be in a very good agreement with the analytical value  $\gamma = 1/(\mu + 1)$ .

The fitted scaling function for the size distributions of the form  $Ax^\delta \exp(-ax)$  is plotted in Figure 2 together with the simulation data with  $(\mu, \alpha) = (2, 0)$ . Similar behaviour with the exponent values  $\delta$  given in Table 1 was found for other combinations of  $(\mu, \alpha)$ . The coefficients  $A = a^{\delta+1}/\Gamma(\delta + 1)$  and  $a = \delta + 1$  follow from the normalization conditions  $\int g(x)dx = 1$  and  $\int xg(x)dx = 1$ , where  $\Gamma(\delta)$  is the gamma function. The latter normalization is derived by inserting the scaling ansatz to the definition of  $\bar{s}$  used here. Thus the scaling function is specified completely with only one parameter  $\delta$ , once the homogeneity exponents  $(\mu, \alpha)$  of the reaction kernels are given. In reference [10] it was suggested that for  $x \gg 1$  all scaling functions collapse into a single curve, independent of  $a$ . The data collapse is obtained for all coverages, and the analytical prediction  $\delta = \mu + \alpha + 1$  is in good agreement with the simulations. The inset shows the unscaled size distributions  $n_s$  with the coverages 0.05, 0.15, and 0.25 monolayers.

In reference [10] some of the results were still tentative and some open questions remained, such as analytical predictions for the scaling exponents and the dependence of the scaling function of the homogeneity exponents in the  $x \gg 1$  regime. Now with the improved computational method, a much broader range of parameter values and better statistics are obtained, and good agreement with the mean field predictions is established. The revised PCM is clearly faster than the old PCM. For example, with  $\mathcal{R} = 10^8$  and  $\kappa = 0$  (only island aggregation), the ratio in CPU-time is 2000 in favor of the revised PCM. The

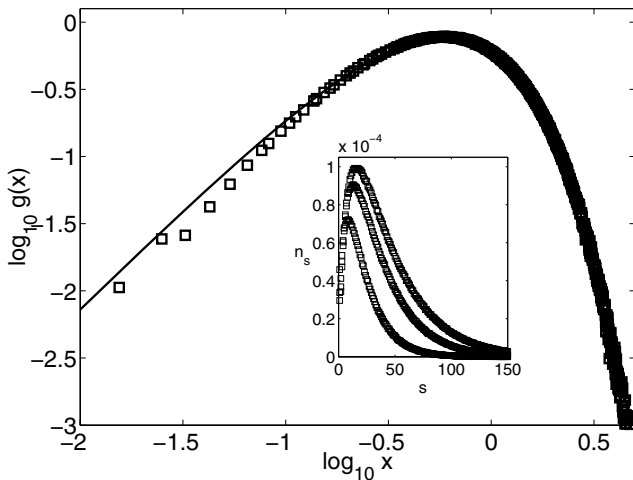


**Fig. 2.** The scaling function  $g(x) = Ax^\delta \exp(-ax)$  is plotted with the fitted  $\delta$  (solid line) against the simulation data (squares) in the case  $(\mu, \alpha) = (2, 0)$  with  $\mathcal{R} = 10^7$ ,  $\kappa = 10^{-5}$ , and  $L = 500$ . The inset shows the real size distributions with the coverages  $\theta = 0.05, 0.15$ , and  $0.25$  (from bottom to top). The coefficients  $A$  and  $a$  are given in the text.

performance of the new method, however, decreases with the increasing fragmentation rate, still remaining faster than the old one. This is due to the fact that only aggregation events are conducted faster in the revised PCM, and with large  $\kappa$  the relative importance of fragmentation events with respect to aggregation events increases. For example, with  $(\mu, \alpha) = (1, -1/2)$ ,  $\mathcal{R} = 10^6$ , and  $\kappa = 10^{-3}$  the ratio in CPU-time is 40 in favor of the new method.

## 5 Conclusions

Island growth with aggregation, fragmentation, and deposition was studied with generalized rate equations. Analytical estimates for the scaling exponents of the mean island size and the size distributions were derived from the rate equations. In the model, island fragmentation and aggregation were characterized by reaction rates with homogeneous kernels with exponents  $\alpha$  and  $\mu$ , respectively.

It was shown that initially growth proceeds with the dynamic exponent  $\beta = 2/(\mu + 1)$ , while the growth exponent is given by  $\gamma = \beta/2$ . In the final quasi-stationary state the mean island size scales as  $\bar{s} \sim \theta^y$  with  $y = 1/(\mu + \alpha + 2)$ . In this region of growth the probability distribution, that an adatom is contained in an island of size  $s$ , scales as  $g(x) \sim x^\delta \exp(-ax)$  with  $\delta = \mu + \alpha + 1$ . These analytical predictions were obtained in the mean-field approximation, and they were confirmed by the numerical integration of the equation of the mean island size. An independent comparison was made with the particle coalescence simulations using the revised method, and good agreement was found in all cases studied.

The revised simulation method developed here enabled us to simulate a large enough regime of the parameter space in order to obtain the island size distributions with small enough statistical errors. We were able to show that

the size distributions are of the scaling form and to characterize the corresponding scaling exponents. The new method could be also used in other systems where numerical integration of the large set of coupled differential equations is not practical.

The good agreement between the analytical predictions and the simulation results show that the scaling exponents for the mean island size and the size distributions depend in a unique way on the homogeneity exponents of the reaction kernels. These findings suggest that it is possible to obtain rather detailed information about microscopic surface processes by examining the scaling properties of island size distributions and the mean island size.

This work was supported by Academy of Finland through the Project 73642.

## References

1. J.A. Venables, *Philos. Mag.* **27**, 697 (1973); J.A. Venables, Hanbuücken, *Rep. Prog. Phys.* **47**, 399 (1984)
2. M.C. Bartelt, J.W. Evans, *Phys. Rev. B* **46**, 12675 (1992)
3. G.S. Bales, D.C. Chrzan, *Phys. Rev. B* **50**, 6057 (1994); *Phys. Rev. Lett.* **74**, 4879 (1995)
4. P.L. Krapivsky, J.F.F. Mendes, S. Redner, *Eur. Phys. J. B* **4**, 401 (1998); P.L. Krapivsky, J.F.F. Mendes, S. Redner, *Phys. Rev. B* **59**, 15 950 (1999)
5. L. Kuipers, R.E. Palmer, *Phys. Rev. B* **53**, R7646 (1996)
6. P.A. Mulheran D.A. Robbie, *Phys. Rev. B* **64**, 115402 (2001)
7. G.S. Bales, D.C. Chrzan, *Phys. Rev. B* **50**, 6057 (1997); C. Ratsch, A. Zangwill, P. Smilauer, D.D. Vvedensky, *Phys. Rev. Lett.* **72**, 3194 (1994)
8. J.M. Pomeroy, J. Jacobsen, C.C. Hill, B.H. Cooper, J.P. Sethna, *Phys. Rev. B* **66**, 235412 (2002)
9. J. Jacobsen, B.H. Cooper, J.P. Sethna, *Phys. Rev. B* **58**, 15847 (1998)
10. I. Koponen, M. Rusanen, J. Heinonen, *Phys. Rev. E* **58**, 4037 (1998)
11. M. Kalf, M. Breeman, M. Morgenstern, T. Michely, G. Comsa, *Appl. Phys. Lett.* **70**, 182 (1997); S. Esch, M. Bott, T. Michely, G. Comsa, *Appl. Phys. Lett.* **67**, 3209 (1995); S. Esch, M. Breeman, M. Morgenstern, T. Michely, G. Comsa, *Surf. Sci.* **365**, 187 (1996); T. Michely, G. Comsa, *Phys. Rev. B* **44**, 8411 (1991); T. Michely, C. Teichert, *Phys. Rev. B* **50**, 11156 (1994)
12. B. Degroote, A. Vantomme, H. Pattyn, K. Vanormelingen, *Phys. Rev.* **65**, 195401 (2002)
13. S.V. Khare, N.C. Bartelt, T.L. Einstein, *Phys. Rev. Lett.* **75**, 2148 (1995); S.V. Khare, T.L. Einstein, *Phys. Rev. B* **57**, 4782 (1998); J. Heinonen, I. Koponen, J. Merikoski, T. Ala-Nissila, *Phys. Rev. Lett.* **82**, 2733 (1999)
14. W.W. Pai, A.K. Swan, Z. Zhang, J.F. Wendelken, *Phys. Rev. Lett.* **79**, 3210 (1997); J.-M. Wen, S.-L. Chang, J.W. Burnett, J.W. Evans, P.A. Thiel, *Phys. Rev. Lett.* **73**, 2591 (1994); K. Morgenstern, G. Rosenfeld, B. Poelsema, G. Comsa, *Phys. Rev. Lett.* **74**, 2058 (1995); K. Morgenstern, G. Rosenfeld, G. Comsa, *Phys. Rev. Lett.* **76**, 2113 (1996)
15. A. Wucher, A.D. Bekkerman, N.K. Dzhemilev, S.V. Verkhoturov, I.V. Veryovkin, *Nucl. Instr. Meth. B* **140**,

- 311 (1998); A. Wucher, N.K. Dzhemilev, I.V. Veryovkin, S.V. Verkhoturov, Nucl. Instr. Meth. B **149**, 285 (1999); S. Becker et al., Comp. Mat. Sci. **2**, 633 (1994)
16. P. Blandin, C. Massobrio, P. Ballone, Phys. Rev. Lett. **72**, 3072 (1994)
17. K. Kyuno, G. Ehrlich, Phys. Rev. Lett. **84**, 2658 (2000)
18. S. Liu, L. Bonig, H. Metiu, Phys. Rev. B **52**, 2907 (1995); M.C. Bartelt, S. Gunther, E. Kopatzki, R.J. Behm, J.W. Evans, Phys. Rev. B **53**, 4099 (1996); I. Furman, O. Biham, Phys. Rev. B **55**, 7917 (1997)
19. P. Meakin, M.H. Ernst, Phys. Rev. Lett. **60**, 2503 (1988)
20. K. Kang, S. Redner, Phys. Rev. A **30**, 2833 (1984); Phys. Rev. Lett. **52**, 955 (1984); K. Kang, S. Redner, P. Meakin, F. Leyvraz, Phys. Rev. A **33**, 1171 (1986)
21. H. Wright, D. Ramkrishna, Phys. Rev. E **47**, 3225 (1993)
22. L. Bitar, P.A. Serena, P. García-Mochales, N. García, V.T. Binh, Surf. Sci. **339**, 221 (1995)
23. J. Sillanpää, I. Koponen, Nucl. Instr. Meth. B **142**, 67 (1998)
24. J.G. Amar, F. Family, P.-U. Lam, Phys. Rev. B **50**, 8781 (1994)
25. C.M. Sorensen, H.X. Zhang, T.W. Taylor, Phys. Rev. Lett. **59**, 363 (1987); R.D. Vigil, R.M. Ziff, Phys. Rev. Lett. **61**, 1431 (1988)
26. E. Adam, L. Billard, F. Lançon, Phys. Rev. E **59**, 1212 (1999)